Resonant vibrational excitation of CO by low-energy electrons

G. B. Poparić* and D. S. Belić
Faculty of Physics, University of Belgrade, Studentski trg 12-16, P.O. Box 368, 11000 Belgrade, Serbia

M. D. Vićić
Washington University School of Medicine, 4921 Parkview Place, Campus Box 8224, St. Louis, Missouri 63110-1093, USA
(Received 15 March 2006; published 16 June 2006)

Electron impact vibrational excitation of the CO molecule, via the $^2\Pi$ resonance, in the 0–4 eV energy region has been investigated. The energy dependence of the resonant excitation of the first ten vibrational levels, $v=1$ to $v=10$, has been measured by use of a crossed-beams double trochoidal electron spectrometer. Obtained relative differential cross sections are normalized to the absolute values. Integral cross sections are determined by using our recent results on scattered electrons angular distributions, which demonstrate clear *p*-partial wave character of this resonance. Substructures appear in the $^2\Pi$ resonant excitation of the CO molecule which have not been previously observed.

DOI: 10.1103/PhysRevA.73.062713 PACS number(s): 34.80.Gs

I. INTRODUCTION

Vibrational excitation of the ground state of CO molecule by electron impact has been long and intensively studied in the past few decades [1,2]. A pronounced resonant contribution of the $^2\Pi$ shape resonance to this process was first observed by Schulz [3] and Ehrhardt *et al.* [4]. The unusual behavior of the excitation cross sections, as in N_2—in particular, the position and widths of the quasi-vibrational resonant structures as a function of excitation channel—was first described by the introduction of the boomerang model, from Birtwistle and Herzenberg [5].

Relative differential cross sections (DCSs) and angular distributions of inelastically scattered electrons from CO, in the energy region from 0.6 to 5 eV, have been measured by Ehrhardt *et al.* [4] for excitation of $v=1-7$ vibrational levels and by Jung *et al.* [6] for resolved rotational excitation. Angular distribution measurements are performed in the range from 20° to 110°. Obtained results show a predominantly *p*-type behavior of the curves, with a minimum at 90°. A fairly good fit to the experimental curves was obtained by O'Malley and Taylor [7], and gives the angular distribution in the form $(1+7\cos^2\theta)$. Read [6] improved the fit to the angular distribution, including asymmetry, by using a mixture of $p\pi$ and $d\pi$ partial waves. The mixing proportion of these two waves is left as a parameter which is adjusted until a good agreement with experimental angular distribution is achieved.

DCSs for excitation of the first vibrational level $(v=0\rightarrow 1)$ of CO have been reported by Land [8], as a result of swarm experiments, by Chutjian and Tanaka [9] and by Sohn *et al.* [10]. More recently, Middleton *et al.* [11] and Gibson *et al.* [12] have also reported DCSs for this transition at energies between 1 and 50 eV. In all of these cases, experimental results are reported for scattering angles up to 130°. Theoretical calculations have been performed in Born dipole approximation (BDA) by Sohn *et al.* [10], *R*-matrix calculations by Morgan and Tennyson [13] and by Morgan [12]. It has been pointed out by Brunger and Buckman [2] that, near the resonance maximum, experimental data agree with each other fairly well but are not reproduced very well by the theory.

Both, experimental results and theoretical predictions show a minimum of the angular distribution at 90 degrees. There is a notable difference in forming the $^2\Pi$ shape resonance, in the isoelectronic molecules CO and N_2. In the case of N_2, the symmetry arguments allow only *d*-partial wave to take place in forming the barrier. The heteronuclear CO molecule has reduced symmetry and its $3d\pi$ orbital allows also a *p*-partial wave component to take place in this resonant scattering process, Read [14]. Observed structure in CO has larger width than in N_2. This is the result of the resonance barrier being of a *p*-wave character (which is not as high as *d* wave barrier and has shorter lifetime) in CO, with the *d* wave mixed in. The mixing of *p* and *d* partial wave contributions in this resonance allows DCS to be asymmetric relative to 90°. This asymmetry is more pronounced in theoretical results, in favor of low scattering angles. The lack of experimental results in the region between 130° and 180° did not allow one to make definite conclusions about this asymmetry or degree of asymmetry. From these reasons, we have recently performed measurements of the ratio of DCS at forward and backward direction, by use of our double trochoidal electron spectrometer with the time-of-flight technique, Poparić *et al.* [15]. We have determined this ratio to be equal to 1 and thus angular distribution to be symmetric around 90°, e.g., clear *p*-partial wave character of scattering process. This result will be used here in order to determine integral cross sections in the resonance energy region.

In our previous high-resolution experiment on vibrational excitation of the isoelectronic N_2 molecule, via the $^2\Pi_g$ shape resonance, a clear evidence of the fine "substructures" has been demonstrated [16]. These substructures were theoretically predicted by Huo *et al.* [17] and were also reported by Allan [18]. Similar substructures are expected to be seen also in the case of a CO molecule, since it has a similar electronic configuration and the same mechanism of resonant excitation.

*Electronic address: goran_poparic@ff.bg.ac.yu

The aim of this experiment is to obtain an additional set of relative cross sections for the vibrational excitation of CO below and in the $^2\Pi$ resonance energy region, with high-energy resolution and particular attention to the predicted substructures, to complete differencial cross sections and to determine integral cross sections for ground-state vibrational excitation of the CO molecule.

II. EXPERIMENTAL TECHNIQUES

The present crossed-beams double trochoidal electron spectrometer is similar to the one described by Allan [18,19], Vićić *et al.* [16,20], Asmis and Allan [21], and in particular by Poparić *et al.* [15]. It has been described in detail by Vićić *et al.* [20] and by Poparić *et al.* [15,22] and only a brief outlook will be given here. The electron beam is prepared by using a trochoidal electron monochromator (TEM), Stamatovic and Schulz [23]. The beam is crossed at right angles with the gas beam, introduced by one-dimensional capillary array, aligned along the electron-beam trajectory, in the collision region. After the collision, inelastically scattered electrons are analyzed by use of a double TEM device. Transmission function of this device is scaled as $1/Er$, where Er is the residual electron energy, Vićić *et al.* [16,20]. Inelastically scattered electrons are detected by use of a channel electron multiplier, counted, and the results are stored in an on-line computer.

Due to the presence of a longitudinal magnetic field, needed for the trochoidal electron selectors operation, in the originally designed apparatus the detected signal consists of the sum of electrons inelastically scattered at 0° and 180°. Electrons scattered at 0° travel straight to the analyzer system and to channeltron detector. On the other side, inelastic electrons scattered at 180° move backward along the incident electron-beam trajectory, are reflected on the potential barrier of the monochromator, reach again the collision region, and from there follow the same path as the 0° scattered electrons. Thus, they travel a longer distance and need a longer time to reach the detector. This fact is used to separate these two groups of electrons by recording their time-of-flight spectra. For this kind of measurement, the incident electron beam from the monochromator needs to be pulsed in an appropriate way. In our experiment, electron-beam chopping is enabled by a square-shaped pulse signal of 1.18 MHz from a 20 MHz clock. Square pulses of 50 ns, 2 V high, are separated by 800 ns. This potential keeps the electron beam on during 50 ns of the pulse time and off for the rest of the time. Since the collision can occur only during the pulse on time, the rising time of the pulses can be used as a trigger of the time-to-amplitude converter (TAC). In fact, this signal is used as a stop trigger of the TAC. For the start of the TAC the signal from the channeltron is used. Therefore, each recorded event represents the time difference between electron detection and the next pulse coming from the generator. This inverted configuration has no influence on the results, but increases the detection efficiency of the experiment. Primary beam and elastic forward and backscattered electrons, as well as various other inelastic electrons are eliminated by a magnetic field and a set of electrodes in the analyzer device. For the reflected 180° electrons, it is possible to undergo second scattering from the target molecules, that would result in their loss. This effect has been investigated both in N_2 and CO and has not been seen because of very low target gas density in the present experiment.

In the case of slow electrons, the time difference between detection of forward and backward electrons is sufficient to separate two contributions. For faster, more energetic electrons, however, backward scattered electrons reflect quickly and follow very closely forward scattered ones and the two contributions overlap in time. Thus, electrons scattered backward with higher-energy need to be decelerated. For this purpose a decelerator device, Poparić *et al.* [15], has been introduced between the end of the monochromator and the collision region. It consists of two parallel plates, 20 mm long. They are kept at low negative potential below the interaction region so that backward scattered electrons travel with low velocity back and forth over this distance and spend some 80 to 100 ns in this device before entering again the collision region from the opposite direction and move further to the detector.

The signal from the channeltron is processed by a fast charge amplifier, voltage amplifier, and high-voltage filter. Obtained pulses are used for the start signal of the TAC. The signal from the TAC is loaded to a pulse-height analyzer and multichannel analyzer. Obtained time-of-flight spectra are analyzed by an on-line computer. This mode of operation of the experiment is used to obtain the ratio of forward to backward DCS. On the other hand, when recording excitation function spectra for particular vibrational levels, electron-beam modulation is disabled and deceleration device is kept at the ground potential of the collision region. In this case all electrons are detected simultaneously.

Particular attention has been devoted to improve the energy resolution of the experiment with the result that a high-energy resolution, below 20 meV full width at half maximum, has been obtained. This has been achieved by "visual" tuning of the selected resonant feature spectrum recorded and displayed repeatedly in short time intervals.

III. EXPERIMENTAL RESULTS AND DISCUSSION

We have measured the excitation functions from $v=0$ of the ground state of CO to the first ten vibrationally excited states ($v=1-10$) via the $^2\Pi$ resonance. In these measurements, electron-beam modulation is disabled and deceleration device is kept at the ground potential. Relative differential cross sections are obtained. In this case all electrons, forward and backward scattered, are detected simultaneously. The acceptance solid angle of the analyzer changes for different residual energy, but this difference is accounted for through the transmission function $1/Er$ correction. A fraction of backward scattered electrons cornerstones to the same solid angle due to the geometrically symmetric forward and backward experimental parameters, and we have assumed that the ratio of forward and backward scattered electrons should be constant for the same vibrational level.

The results of our measurements are presented in Fig. 1(a), together with the experimental results of Allan [19],

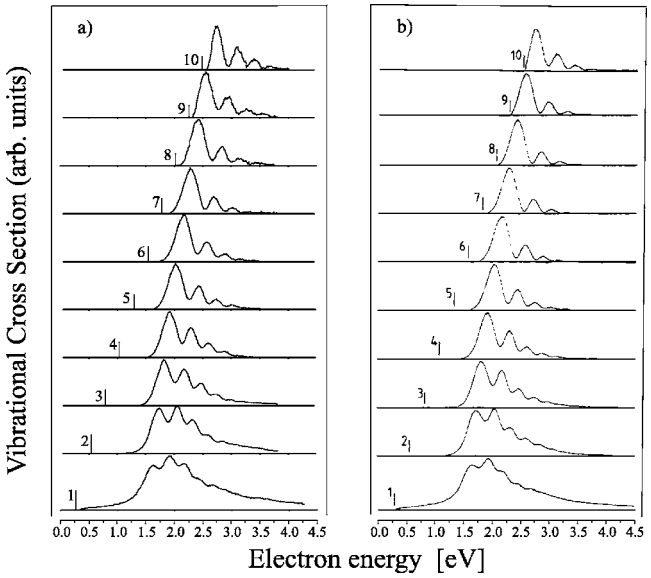

FIG. 1. Excitation functions for vibrational levels 1–10; column (a)—present data, column (b)—adopted from Allan [19].

Fig. 1(b), for comparison. Relative cross sections versus incident electron energy are presented and all curves are normalized to the unity at their maximum. These results are obtained with disabled deceleration device and represent the sum of forward and backward scattered electrons. The vertical bars on the left indicate the corresponding threshold energies, coinciding with the zero energy of the residual electron energy scale in the same units as incident energy. Generally, two sets of data agree very well with each other as to the energy positions of the peaks, their relative magnitude, and energy shifts of the higher vibrational levels. However, some differences between these two sets of data will be pointed out.

For the first curve, $v=1$, the valleys between the peaks are slightly deeper in Fig. 1(a) than those measured by Allan, Fig. 1(b), same as for $v=2$. Some of peaks in our measurements are more asymmetric than were measured by Allan, in particular for $v=5$, 8, and 9. Particular attention should be focused on the $v=8$ and $v=9$ curves. In Fig. 1(b), the first peaks for these two levels are more or less smooth and symmetric. Our results for these two levels indicate the possible substructure of these peaks. This will be discussed later in this text.

In order to resolve relative differential cross sections at 0° and 180°, we have used the procedure described in our recent measurements [15] in time-of-flight mode of spectrometer operation. The ratio of forward to backward DCS in the case of $^2\Pi$ resonant excitation of the CO molecule is found to be equal to (1.00 ± 0.06), for all vibrational levels.

Obtained results are compared with existing measurements of the relative DCSs of Gibson *et al.* [12] in the region from 15° to 130°, for $v=1$ level. Theoretical predictions for angular distribution of scattered electrons proposed by Read [14] for heteronuclear diatomic molecules are used to normalize our results to Gibson *et al.*'s [12] data. Type I resonance (Read [14]) is considered with contributions of $p\pi$ and $d\pi$ waves. The following expression, with two fitting parameters, ρ and γ, is used in the form:

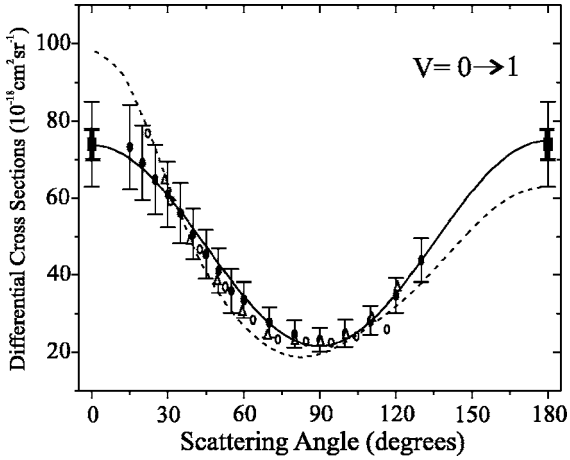

FIG. 2. Angular distribution of electrons from $^2\Pi$ resonant excitation of CO at 1.91 eV. Points at 0° and 180° are our data, closed circles are of Gibson *et al.* [12], open circles are of Ehrhardt *et al.* [4], triangles are of Tronc *et al.* [24], solid curve is the fit with Eq. (1) and dashed line theory are of Morgan [12]

$$\mathrm{DCS} = C[(0.03333 + 0.04286\rho^2 + 0.08571\rho) + \cos\theta(-0.28571\rho\cos^2\gamma) + \cos^2\theta(0.23333 - 0.12857\rho^2 + 0.14286\rho)]. \quad (1)$$

This formula is used to fit the data of Gibson *et al.* [12], from 15° to 120°, with our results of equal values at 0° and 180°. The best fit is obtained with asymmetry parameter $\cos^2\gamma=(0.013\pm0.010)$, which is essentially zero, and $\rho=(0.68\pm0.03)$. The normalization constant, C, for the $v=1$ level excitation is found to be $(194\pm3)10^{-18}$ cm^2 sr^{-1}. Absolute DCS values at 0° and at 180° are found to be $(74\pm9)\ 10^{-18}$ cm^2 sr^{-1}.

The obtained fit is shown by solid line in Fig. 2. Our data at 0° and 180° are shown by solid squares and data of Gibson *et al.* [12] are shown by solid circles. Experimental data of Ehrhardt *et al.* [4], open circles; and Tronc *et al.* [24], triangles, are also shown in Fig. 2. Theoretical predictions of Morgan *et al.* [12] are shown in the Fig. 2 by dashed line, but they disagree with all experimental results at low scattering angles.

Total absolute uncertainties of our data are obtained by quadrature sum of our statistical uncertainties of 5% and absolute uncertainty of Gibson *et al.* [12] measurements to which normalization has been performed. In Fig. 2, we have shown our relative uncertainties by thick error bars, and absolute uncertainties by thin ones. As can be seen from Fig. 2, all experimental data agree well that this angular distribution is fully symmetric around 90°. According to Read [14], this conclusion supports the fact that the contribution of the $p\pi$ partial wave is dominant in the energy region of $^2\Pi$ resonance in CO.

DCSs for all other vibrational levels are normalized by using their relative count rate under the same experimental conditions, i.e., gas pressure, electron-beam current, residual electron energy, and signal accumulation time. Obtained results are presented in Table I. By taking into account the angular distribution of scattered electrons Eq. (1) and DCSs

TABLE I. Energy position, DCS ratio, DCSs, and ICS at the maximum for the first ten vibrational levels of excitation.

v	Electron energy	DCS ratio	Ratio of Allan[a]	DCS at 0° 10^{-17} cm^2 sr^{-1}	ICS 10^{-16} cm^2
1	1.91	1.00	1.00	7.40	4.88
2	2.03	0.47	0.33	3.48	2.29
3	1.79	0.25	0.17	1.85	1.22
4	1.90	0.16	0.11	1.18	0.78
5	2.01	0.10	0.073	0.74	0.49
6	2.14	0.061	0.042	0.45	0.30
7	2.25	0.032	0.024	0.236	0.156
8	2.42	0.014	0.012	0.104	0.068
9	2.55	0.006	0.005	0.047	0.031
10	2.73	0.002	0.002	0.014	0.009

[a]See Allan [19]

at 0° obtained in our normalization procedure for each vibrational level, we have estimated integral cross sections for electron impact excitation of the first ten vibrational levels, at the cross-section maximum. Obtained results are also shown in Table I.

Energy positions of the cross-section maxima of our data are in excellent agreement with the data listed by Allan [19]. The difference is within 10 meV. However, these values are for about 0.1 eV lower in measurements of Ehrhardt *et al.* [4], it seems that their energy scale is shifted for this amount toward lower energies.

The ratios of the particular DCS relative to the DCSs for $v=1$ are listed in Table I for our data and for data of Allan [19], the latter being somewhat lower for all vibrational levels. Discussed ratios are extremely sensitive to the energy resolution and tuning of the experiment. By use of our visual tuning technique, we are able to isolate the $v=1$ inelastic peak completely from the elastic scattering. Mixing of the two contributions may lower the discussed ratios. The data of Ehrhardt *et al.* [4], taken from their figures, are in better agreement with our data. This comparison is shown schematically in Fig. 3.

In Table I, we have also listed absolute DCSs at 0° and obtained integral cross-section (ICS) values at the cross-section maximum for the first ten vibrational levels. As we just pointed out, our DCS at 0° for $v=1$ is found to be (7.4 ± 9) 10^{-17} cm^2 sr^{-1}. This is consistent with the data of Gibson *et al.* [12] since our data are normalized to their DCSs. Their value taken at 15° is 7.32×10^{-17} cm^2 sr^{-1}. This is also in a good agreement with the data of Ehrhardt *et al.* [4]. DCSs of Jung *et al.* [6] are higher for all angles for 30–40%, and at 15° they have obtained value of 1.2×10^{-16} cm^2 sr^{-1}, which is significantly higher than our and any other reported value.

Selected ICS values are also listed in Table I. For $v=1$, we have obtained an ICS value of 4.88×10^{-16} cm^2. This is in excellent agreement with the value of 4.874×10^{-16} cm^2 given by Gibson *et al.* [12]. The ICS value of Ehrhardt *et al.* [4] at the maximum for $v=1$ level excitation, at 1.8 eV, is 3.4×10^{-16} cm^2, some 30% lower than the above-mentioned

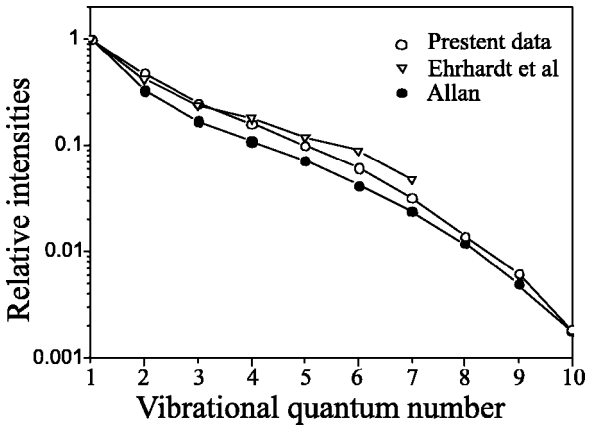

FIG. 3. Relative DCSs at 0° at the maximum versus vibrational level quantum number. Open circles are present data, triangles are data of Ehrhardt *et al.* [4], and closed circles are data of Allan [19].

values. In Fig. 4, we have compared our ICS values for $v=1$ with other available experimental and theoretical data. Open circles are present data, solid squares are data of Gibson *et al.* [12], solid curve is the *R*-matrix theory of Morgan [12], triangles are data of Sohn *et al.* [10], semidashed line is the BDA theory [10], dashed curve is *R*-matrix theory of Morgan and Tennyson [13], and solid circles are data from Chutjian and Tanaka [9]. As can be seen from Fig. 4, the agreement is very good in the near-maximum energy region.

ICSs for the first ten vibrational levels are shown versus electron energy in Fig. 5, on a semilog scale. Values at the cross-section maxima are listed in Table I for each vibrational level. The sum of ICSs for all vibrational levels is also shown in Fig. 5, and it represents the total ICSs for vibrational excitation via the $^2\Pi$ resonance. It has a maximum value of 8.54×10^{-16} cm^2 at an electron energy of 1.94 eV.

We will bring our attention back again to the form of obtained spectra. In the papers of Huo *et al.* [17] and Vićić *et al.* [16], a fine substructure of $^2\Pi_g$ resonant excitation of the nitrogen molecule has been demonstrated and discussed. The substructures are connected primarily to the first peak of the spectra, i.e., to the first quasi-vibrational level of the resonant state. In this work, we have searched for the same feature in the $^2\Pi$ resonant excitation of the CO molecule.

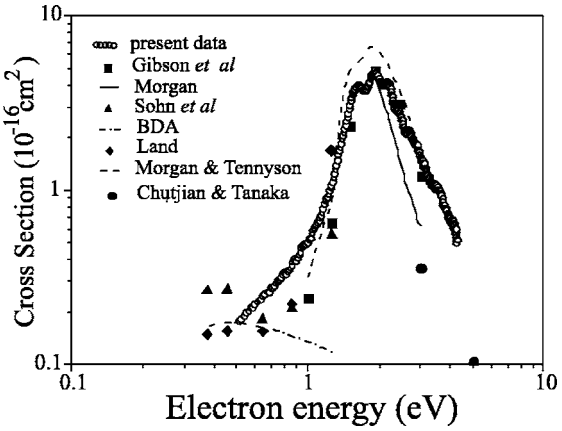

FIG. 4. Comparison of ICSs for $v=1$ excitation channel.

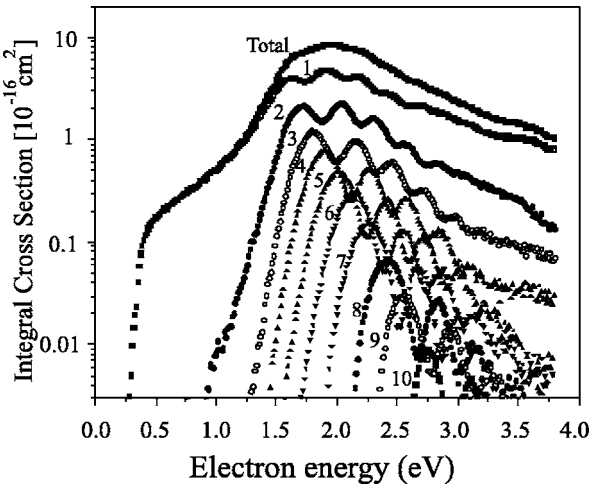

FIG. 5. Total and partial ICSs for vibrational excitation of CO.

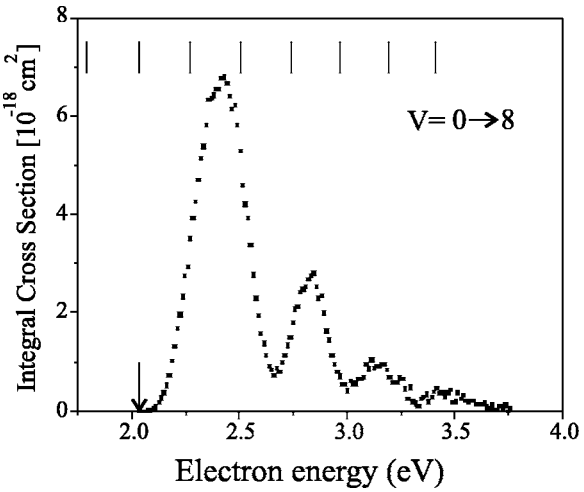

FIG. 7. ICS for excitation of $v=8$ vibrational level.

Measurements are performed with the same experimental device and under the same conditions of high-energy resolution. Obtained results are not as clear as in the nitrogen case, Vićić *et al.* [16]. However, some asymmetries of peaks and possible substructures can be seen in the CO case, as well. This is illustrated in Figs. 6–8.

In Figs. 6–8, and ICSs for $v=5$, 8, and 9 level excitation are shown in details. It can be seen from Fig. 6. that the first peak is sharply pointing up; showing changes of the slope at its both sides, a feature which is not present in other cases. On the other hand, both first and second peaks of $v=8$ and $v=9$ vibrational level excitation are somewhat broadened indicating a weak substructure or cut in the peak shape. Similar features in the nitrogen molecule were more pronounced.

In order to explain this feature, we have primarily searched for the energy scheme which could lead to the substructures. In Figs. 6–8, energies of the ground-state higher vibrational levels are indicated by the vertical bars together with the excitation functions for $v=5$, 8, and 9 levels. As can be seen from the figures, some higher vibrational levels of the ground state of the neutral molecule coincide very well with the positions of the substructures in $v=5$, 8, and 9 excitation channels.

This near-degeneracy presumably leads to the nonadiabatic mixing of two states, one of which is (long-lived) resonant, while the other is well-defined vibrational level of the neutral molecule, and therefore results in the observed decrease of the cross section. The meaning of nonadiabatic in this context is referred to the Born-Oppenheimer approximation. This obviously needs to be further theoretically investigated in detail. The reason for a weaker substructure in CO than in the nitrogen case should be attributed to the shorter lifetime of $^2\Pi$ resonance in CO and, consequently, the closer spacing of the quasi-vibrational structure in CO molecule.

IV. CONCLUSIONS

Relative DCSs for low-energy electron impact vibrational excitation of the CO molecule have been measured, by using a crossed-beam double trochoidal electron spectrometer with high resolution. Obtained spectra are normalized to the

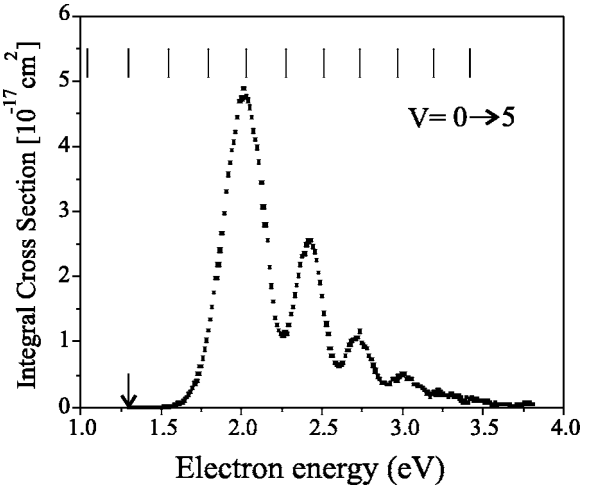

FIG. 6. ICS for excitation of $v=5$ vibrational level.

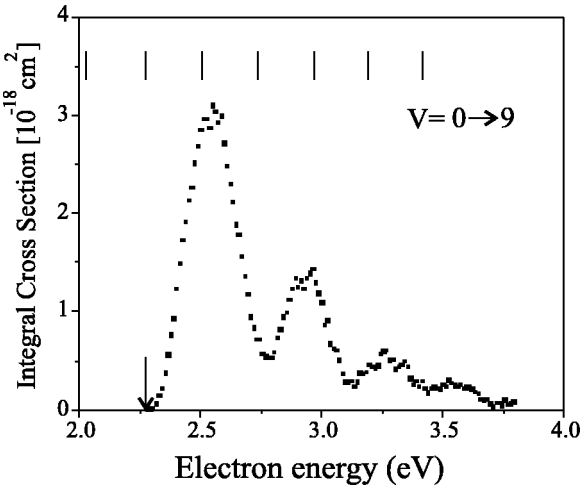

FIG. 8. ICS for excitation of $v=9$ vibrational level.

absolute scale. ICSs for the first ten vibrational levels are determined. Characteristic substructure in energy excitation spectra has been obtained and discussed for some vibrational channels.

ACKNOWLEDGMENTS

This work was supported in part by the Ministry of Science of the Republic of Serbia, under Project No. 141015.

[1] G. J. Schulz, Rev. Mod. Phys. **45**, 423 (1973).
[2] M. J. Brunger and S. J. Buckman, Phys. Rep. **357**, 215 (2002).
[3] G. J. Schulz, Phys. Rev. **136**, A650 (1964).
[4] H. L. Ehrhardt, L. Langhans, F. Linder, and H. S. Taylor, Phys. Rev. **173**, 222 (1968).
[5] D. T. Birtwistle and A. Herzenberg, J. Phys. B **4**, 53 (1971).
[6] K. Jung, T. Antoni, R. Muller, K.-H. Kochem, and H. Ehrhardt, J. Phys. B **15**, 3535 (1982).
[7] T. F. O'Malley and H. S. Taylor, Phys. Rev. **176**, 207 (1968).
[8] J. E. Land, J. Appl. Phys. **49**, 5716 (1978).
[9] A. Chutjian and H. Tanaka, J. Phys. B **13**, 1901 (1980).
[10] W. Sohn, K. H. Kochem, K. Jung, H. Ehrhardt, and E. S. Chang, J. Phys. B **18**, 2049 (1985).
[11] A. G. Middleton, M. J. Brunger, and P. J. O. Teubner, J. Phys. B **25**, 3541 (1992).
[12] J. C. Gibson, L. A. Morgan, R. J. Gulley, M. J. Brunger, C. T. Bundschu, and S. J. Buckman, J. Phys. B **29**, 3197 (1996).
[13] L. A. Morgan and J. Tennyson, J. Phys. B **26**, 2429 (1993).
[14] F. H. Read, J. Phys. B **1**, 893 (1968).
[15] G. B. Poparić, S. M. D. Galijaš, and D. S. Belić, Phys. Rev. A **70**, 024701 (2004).
[16] M. Vićić, G. Poparić, and D. S. Belić, J. Phys. B **29**, 1273 (1996).
[17] W. M. Huo, T. L. Gibson, M. A. P. Lima, and V. McKoy, Phys. Rev. A **36**, 1632 (1987).
[18] M. Allan, J. Phys. B **18**, 4511 (1985).
[19] M. Allan, J. Electron Spectrosc. Relat. Phenom. **48**, 219 (1989).
[20] M. Vićić, G. Poparić, and D. S. Belić, Rev. Sci. Instrum. **69**, 1996 (1998).
[21] K. R. Asmis and M. Allan, J. Phys. B **30**, 1961 (1997).
[22] G. B. Poparić, M. D. Vićić, and D. S. Belić, Phys. Rev. A **66**, 022711 (2002).
[23] A. Stamatović and G. J. Schulz, Rev. Sci. Instrum. **39**, 1752 (1968).
[24] M. Tronc, R. Azria, and Y. L. Coat, J. Phys. B **13**, 2327 (1980).